

EGPRS Test: Meeting the Challenge of 8PSK Modulation

Application Note

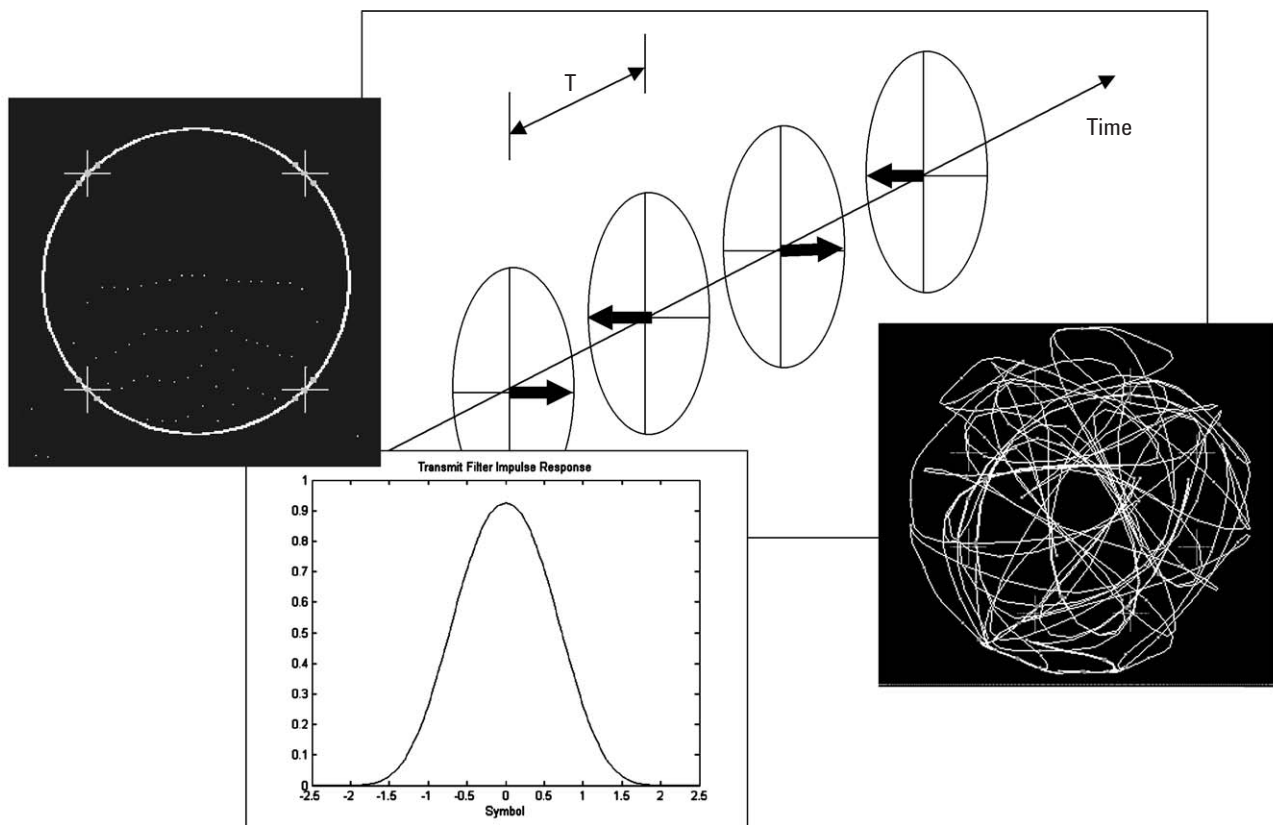


Table of Contents

Overview	2
GMSK and 8PSK Modulation	3
Power Measurement	8
Modulation Accuracy Measurement	13
IQ Modulator Tuning	18
Test Modes	20
Summary	21

Overview

Gaussian minimum shift keying (GMSK) is the modulation format chosen by the European Telecommunications Standards Institute (ETSI) for GSM and GPRS systems. More recently, ETSI adopted an 8PSK modulation format for use in EDGE.

This application note starts with a review of the 8PSK modulation format. The reasons for adopting 8PSK with $3\pi/8$ rotation in the EDGE system are presented. The relationship between GMSK and 8PSK is reviewed.

The challenges of 8PSK power measurements are then considered. The dependence of burst power on modulating data is discussed and quantified. In this context, the trade-off between burst power measurement accuracy and speed is studied. The estimated carrier power concept is introduced as a technique for achieving the required measurement accuracy without having to compromise measurement speed.

From power measurements, we move on to consider the 8PSK modulation accuracy measurements. The manner in which modulation accuracy is specified in the standards reflects the noise-like nature of this measurement. A statistical model is derived to help understand and quantify the rms EVM parameter.

The problem of IQ modulator tuning is addressed. A method for tuning IQ modulators while transmitting normally formatted 8PSK bursts is presented.

The application note concludes with a review of the test modes defined by the standards to support EGPRS mobile test.

GMSK and 8PSK Modulation

In GSM-based digital systems, GMSK is a constant-envelope modulation format used for spectral and power efficiency. It is a special case of frequency shift keying (FSK) modulation and, as such, transfers information by the instantaneous frequency. In GMSK a “1” is represented by a positive shift in frequency away from the carrier signal, and a “0” is represented by a negative shift in frequency away from the carrier.

We can illustrate what happens to the phase of the carrier in the time domain using a phasor (vector) diagram such as the one illustrated in Figure 1. In this case, the modulating data forces the instantaneous phasor to follow the unit circle.

Like analog FM, GMSK is a non-linear modulation format. We can, however, view it as a form of phase shift keying (PSK) and linearize the generation of the GMSK signal.

$$v(t) = v_c \cos(2\pi f_0 t + \phi(t) + \phi_0)$$

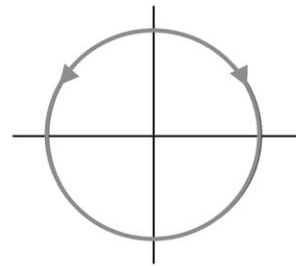
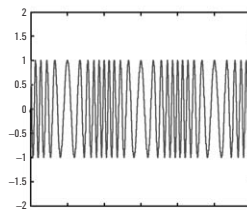


Figure 1. GMSK: a non-linear form of modulation

The first step in linearizing GMSK is to consider the binary phase shift keying system (BPSK). In this system, a “1” is transmitted when the carrier has a phase value of zero and a “0” is transmitted when the carrier has a phase value of π .

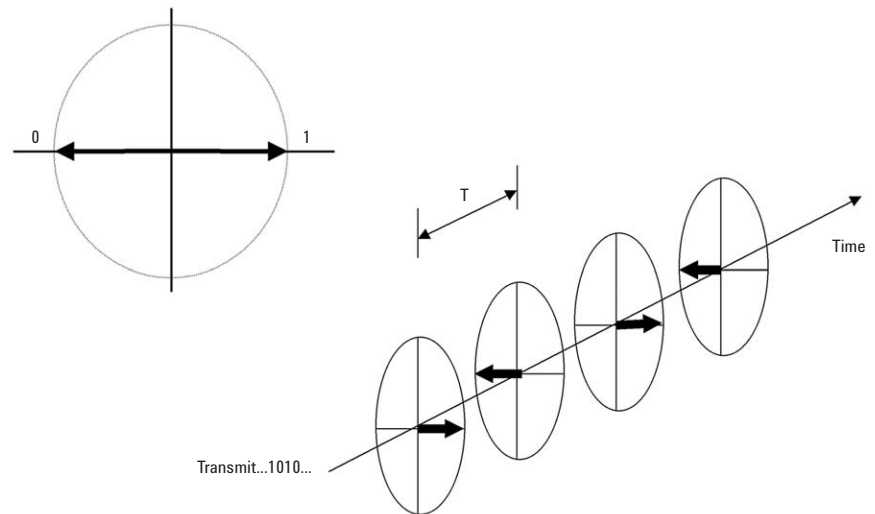


Figure 2. Linearized GMSK

Transmitting a continuous stream of 1s would keep the phasor stationary in the 0 position. To achieve minimum shift keying (MSK), the phasor has to advance by $\pi/2$ radians on each symbol—that is, to rotate 90 degrees around the circle. (See Figure 3.)

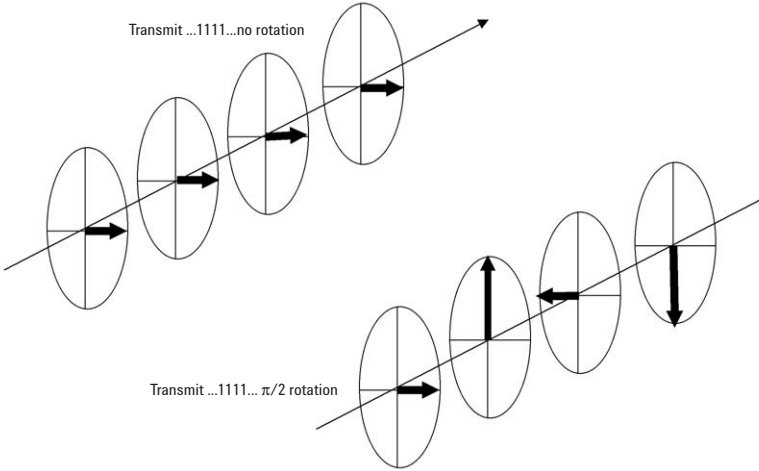


Figure 3. PSK with $\pi/2$ rotation

In this model, the signal is defined only at the symbol points, so between the symbol points, the signal must be interpolated. Moreover, it must be interpolated in such a way that the signal emulates the phase transitions imposed by the Gaussian filter defined in the standards. This interpolation is achieved through a process called Laurent decomposition in which we treat each bit that is to be transmitted as a separate signal, convolve each with an amplitude shaping pulse, and then add together (through superposition) the resulting time-domain responses, which are amplitude-modulated pulses.

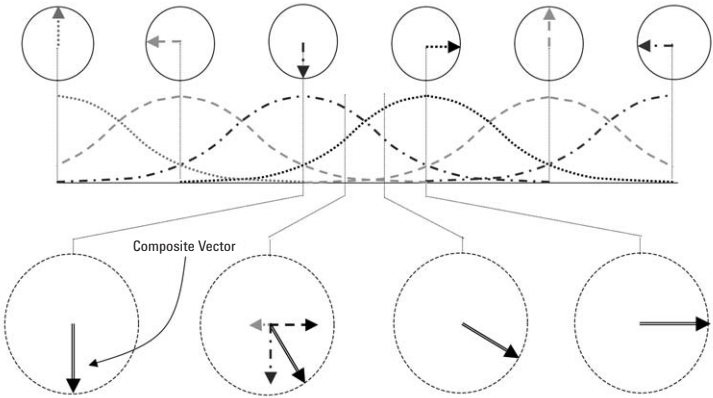


Figure 4. Laurent decomposition

Laurent decomposition is illustrated in Figure 4. Each signal trace in the diagram represents an individual bit, graphed as amplitude versus time to indicate the signal’s time response.

As each signal rises, it reaches a peak that is associated with a symbol point on the phasor diagram, that defines the clock location for that particular bit. When the signal falls, we see a certain amount of time overlap with the next signal. If we add the traces, the power should remain nominally the same at all times because linearized GMSK is also a constant-envelope system.

The GMSK modulation format, designed originally for GSM systems, is also used in GPRS. However, when ETSI began work on the EDGE standard, they were looking for a modulation format that would increase the system's raw data rate. This improvement had to be achieved within certain constraints. Because EDGE and GSM systems would share the same spectrum—in fact, EDGE data slots would be intermixed with GSM voice slots—compatibility in the frequency domain was essential.

8PSK is the modulation format chosen by ETSI for EDGE. The 8PSK format transmits three bits per symbol, in contrast to GMSK, which transmits only one. Through use of the same pulse-shaping filter, however, the spectra of 8PSK and linearized GMSK can be approximately matched.

Another ETSI goal was to minimize the complexity (and cost) of hardware, particularly in the handsets. Consequently, the 8PSK format was designed in such a way that the handset can easily distinguish (without additional signaling) between the 8PSK and GMSK formats. This identification process is called blind detection.

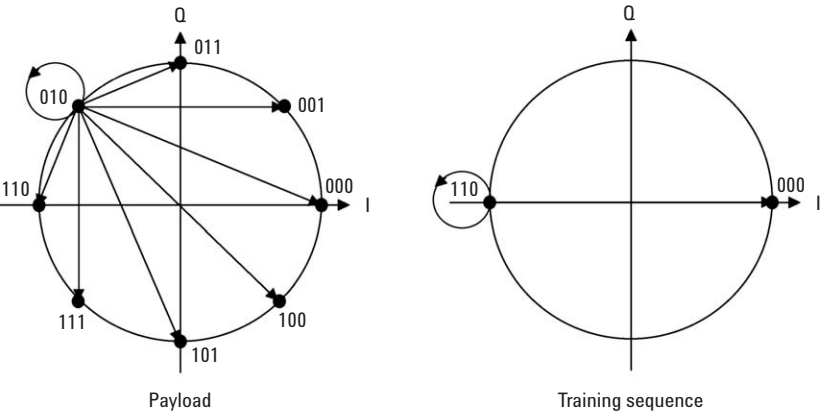


Figure 5. 8PSK modulation

Figure 5 shows 8PSK modulation in its classic form. We see that 8PSK defines eight phase states for the payload and two modulation states for the training sequence. Within the constraints of the payload and training sequence, a signal can move from one state to any other state or stay at the same state.

Looking at the phasor diagrams in Figure 5, we can see that the transition between 010 and 100 in the payload case and between 110 and 000 in the training sequence are problematic. In each of these transitions, the instantaneous vector crosses the origin, which means that the carrier amplitude, which is the length of the instantaneous vector, goes to zero. This puts a requirement for infinite dynamic range on the power amplifier—a problem that we would like to avoid!

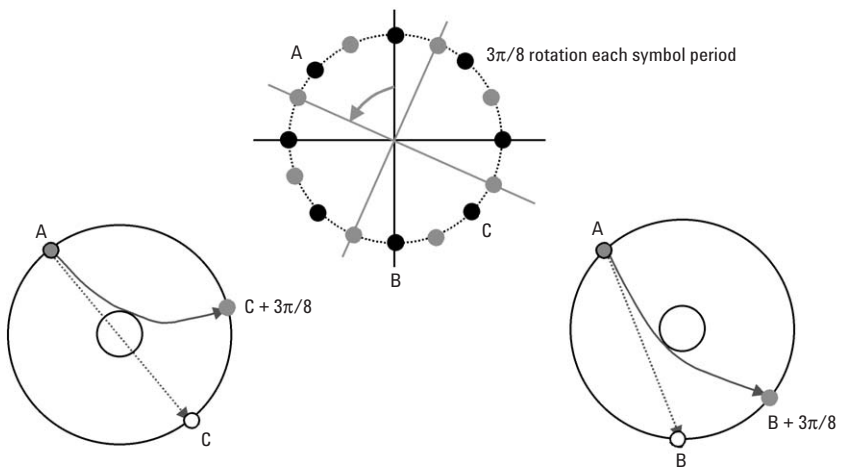
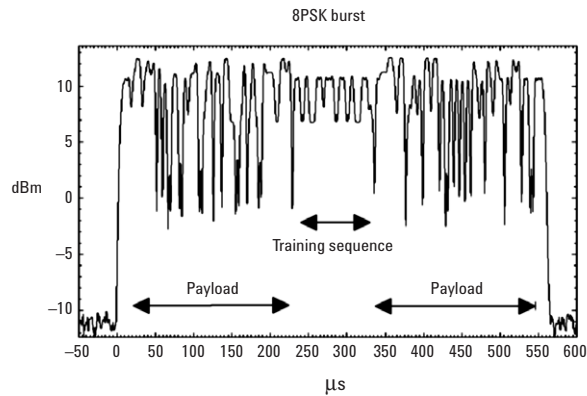


Figure 6. 8PSK modulation with rotation

To resolve the problem, we use $3\pi/8$ rotation in the symbols illustrated in Figure 6. This approach has the effect of creating a kind of “keep out” zone in the center of the circular plot. The symbol rotation steers the instantaneous vector away from the region surrounding the origin. This effectively limits the dynamic range of the symbol.



Rotation	Peak-to-average ratio		Peak-to-minimum ratio	
	Training sequence	Payload	Training sequence	Payload
0	3.4 dB	3.3 dB	∞ dB	∞ dB
$3\pi/8$	1.5 dB	3.2 dB	4.3 dB	16.6 dB

Figure 7. Power ratios

Figure 7 shows a time domain burst of a real 8PSK signal. Note that the rise is not a straight line; it has a shape that is used mainly to control the spectrum during the transition. Next we see the data (payload) portion of the burst, and in the middle we see an area of much lower amplitude where the training sequence occurs. Finally we see the remainder of the data portion of the burst.

The table shows that in the peak-to-average ratio, by using the $3\pi/8$ rotation, we lower the overall value by a small amount during the payload sequence, from 3.4 dB to 1.5 dB, and by a larger amount during the training sequence, from 3.3 dB to 3.2 dB.

Looking at the peak-to-minimum ratio, without symbol rotation the value is infinite because the signals pass through the origin. With $3\pi/8$ rotation, the dynamic range of the payload sequence is limited to 16.6 dB.

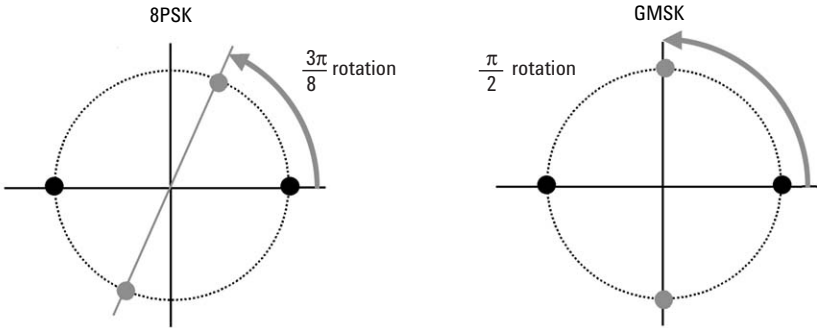


Figure 8. Blind detection

In Figure 8 we see the results of $3\pi/8$ rotation on detection during the training sequence. Recall that only two phase states are used for the training sequence. As a result, the training sequence symbols for GMSK and 8PSK differ only in the degree of rotation: $\pi/2$ for GMSK and $3\pi/8$ for 8PSK. Knowing what the training sequence is, the handset can easily distinguish between the GMSK and 8PSK formats by determining the rotation during the training sequence—the process is known as blind detection.

Power Measurement

One of the difficulties of any system with higher order modulation and non-constant amplitude is that the signal looks like noise. In dealing with noise we are dealing with a statistical process, one which needs to be modeled as accurately as possible. We would also like to measure as quickly as possible.

Before examining this topic in detail, let us look at how the standards define some key terms.

- Burst power is the average power over the useful part of the burst. In other words, rise time and fall time are excluded from our calculation and only the remaining output power is considered. Additionally, burst power is calculated only when the handset is transmitting.
- GSM output power and GSM burst power are the same.
- 8PSK output power is defined as the long-term average of 8PSK burst power.

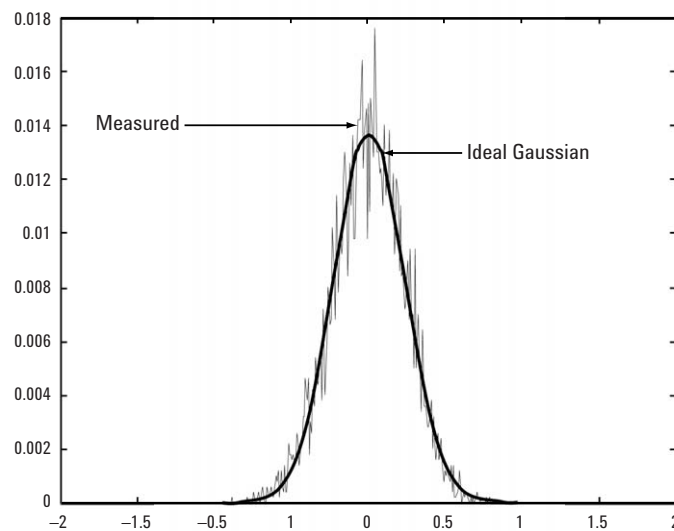


Figure 9. Distribution (PDF) of burst powers

If we were to make many burst power measurements on an 8PSK signal transmitting random data and then plot the results in a histogram format, we would get the bell-shaped distribution illustrated in Figure 9.

The burst power distribution, which is quite uniform, is superimposed over an ideal Gaussian curve. As we can see, there is a good match. The Gaussian distribution thus provides a useful model—well understood and easy to analyze—that can be used to estimate the number of averages required for a given accuracy in our 8PSK burst power measurement.

Taking into account standard deviation, we can derive a method for predicting how long it will take to measure 8PSK burst power to achieve a desired confidence level. Figure 10 shows the range of uncertainty for each of two different confidence levels, calculated as a function of the number of averages. The graph indicates that there is a tradeoff between measurement accuracy and speed. As one might guess, greater confidence requires longer measurement time. The amount of time required for measuring 8PSK burst power is considerably longer than for GSM; possibly too long in terms of the production of a phone.

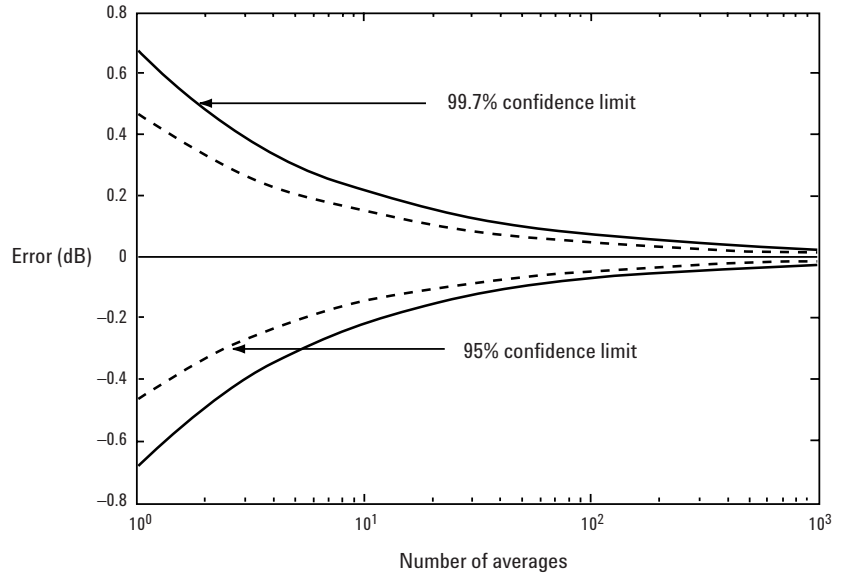


Figure 10. Measurement uncertainty as a function of the number of averages

Agilent has developed an estimated carrier power measurement that avoids having to make the tradeoff between measurement speed and accuracy. This measurement offers considerable practical value in a production test environment.

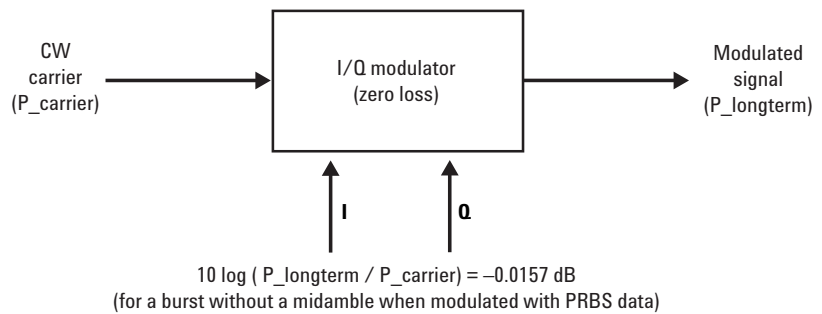


Figure 11. Estimating long-term average power

To develop a useful method of estimating the long-term average of burst power, we must first consider how an 8PSK signal might be generated.

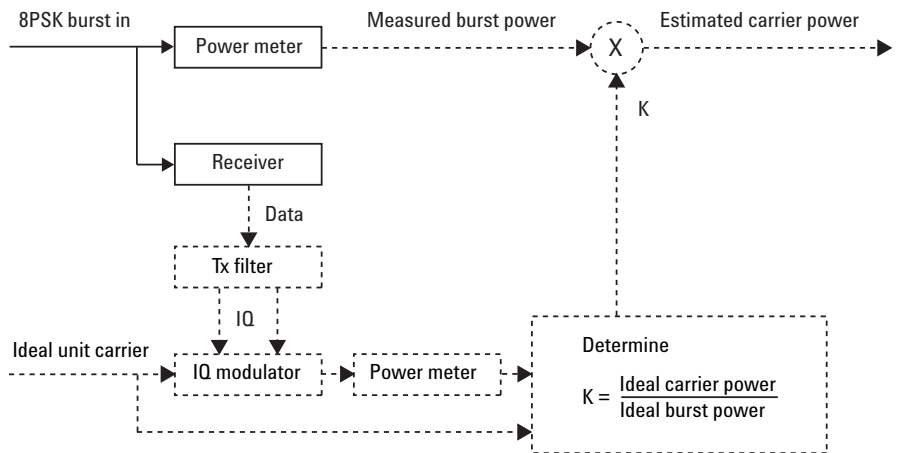
In a typical mobile station output section, modulation is applied to a carrier by means of an I/Q (in-phase and quadrature-phase) modulator. The result is the 8PSK modulated signal as illustrated in Figure 11. The relationship between the carrier signal (P_{carrier}) and the long-term average of the modulated signal (P_{longterm}) is deterministic, and we can see a small shift in power (-0.0157 dB.)

TSC	10 log (P_longterm/P_carrier)
0	0.01 dB
1	0.01 dB
2	0.03 dB
3	0.03 dB
4	0.01 dB
5	-0.01 dB
6	0.03 dB
7	0.06 dB

Figure 12. Long-term average power as a function of training code sequence

When real 8PSK bursts are considered, we observe more variation in the ratio of P_longterm to P_carrier. In all cases, P_carrier provides a good estimate of P_longterm. However, the training sequence used will be a factor in the offset. Because we know which training sequence code (TSC) is being used, we can calibrate out the variation.

Knowing the carrier power, we can predict the long-term average of burst power. It turns out that carrier power can be estimated from a single burst power measurement. This is the principle that underlies the estimated carrier power (ECP) measurement technique used in Agilent's test sets.



Note: Software elements have dashed outline

Figure 13. ECP measurement block diagram

Figure 13 illustrates the ECP measurement technique.

First we make an absolute burst power measurement using a power meter. The same burst is then demodulated in the receiver and the data symbols passed to the digital signal processor (DSP). Conceptually, the transmit path is replicated within the DSP. The received data is used to modulate a unit carrier and the resulting simulated burst power is measured over the same interval as the actual burst power. This allows us to determine the ratio of the ideal carrier power to the ideal burst power for the transmitted data. When the measured burst power is scaled by this ratio (K), we get an estimate of the carrier power.

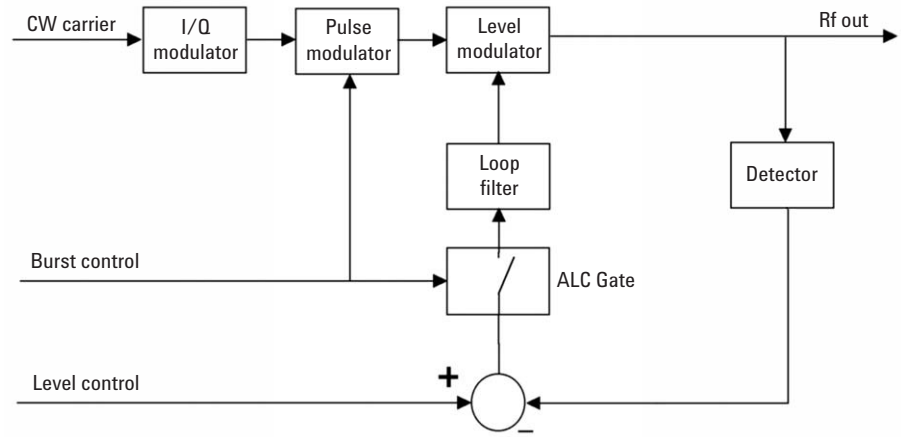


Figure 14. ALC interactions

The effectiveness of this measurement is somewhat dependent on the design of the phone being tested.

A phone typically uses an automatic level control (ALC) loop to level the signal. The design of this loop is often proprietary and not subject to standards, since it does not affect the interface between the phone and the base station. Vendors therefore implement level control in different ways, which are not always known to the test equipment vendor and may therefore have some effect on measurement accuracy.

Figure 14 illustrates one particular design where a gated ALC follows an IQ modulator. Gating prevents the signal from being leveled when the burst is off, but it can be ignored in the present discussion. The purpose of the ALC is to level the output power. It achieves this by maintaining a zero error signal between the level control signal and the detector output. If the output power were to drift, the error signal would no longer be zero. A non-zero error signal drives the level modulator to correct the RF output power so that the zero error condition is restored. In this fashion the ALC compensates for power variations in the signal applied to its input. In Figure 14 the input is an 8PSK-modulated signal. As already discussed, the 8PSK signal exhibits significant power variation across the burst and from burst-to-burst. This represents a power variation that the ALC tries to remove.

If the ALC had sufficient bandwidth, say 300 kHz, all amplitude variation would be removed from the 8PSK signal. In this case the standard deviation in burst power at its output would be zero. Such a scenario is undesirable as the resulting signal could not be properly received. In practice, the ALC bandwidth will be set to a value less than 200 Hz. However, even then, the ALC is capable of removing some of the burst-to-burst power variation, and a reduction in the standard deviation of burst power at the output can be expected.

ALC bandwidth has the reverse effect on the ECP measurement. The ECP measurement sees an ALC-induced correction to burst power as a change in carrier power. The wider the bandwidth, the greater is the capacity of the ALC to level or correct the signal, and consequently, the greater the variation in observed carrier power. Therefore, as the ALC bandwidth increases, the standard deviation of the ECP measurement will also increase.

ALC noise bandwidth	Input burst power standard deviation	Output burst power standard deviation	Output ECP standard deviation
10 Hz	0.23 dB	0.229 dB	0.025 dB
20 Hz	0.23 dB	0.228 dB	0.035 dB
50 Hz	0.23 dB	0.224 dB	0.055 dB
100 Hz	0.23 dB	0.218 dB	0.077 dB
200 Hz	0.23 dB	0.204 dB	0.109 dB

Figure 15. Standard deviation values as a function of ALC noise bandwidth

Figure 15 shows how the standard deviation values of the burst power and the ECP measurements are affected by the ALC noise bandwidth. Adding the squares of the output burst power and output ECP standard deviations will equal the square of the input burst power standard deviation.

Measurement	Burst power	ECP
Required test accuracy	0.50 dB	0.50 dB
Measurement accuracy	0.32 dB	0.40 dB
Allowance for data variation (E_d)	0.18 dB	0.10 dB
100 Hz BW: 3σ	0.65 dB	0.23 dB
$N = \text{Ceil}((3/\sigma E_d)^2)$	14	6
50 Hz BW: 3σ	0.67 dB	0.17 dB
N	14	2
No ALC: 3σ	0.69 dB	0.0 dB
N	15	1

Figure 16. When to use burst power or estimated carrier power

Having calculated the burst power and ECP standard deviations for a given bandwidth, we can proceed to analyze the measurement accuracies to determine how many averages are needed. In the example illustrated in Figure 16, we assume a required test accuracy of 0.5 dB. The basic measurement accuracies are 0.32 dB for the burst power measurement and 0.4 dB for the ECP measurement. This leaves an allowance for data variation of 0.18 dB in the burst power measurement and 0.1 dB in the ECP measurement.

To obtain a 99.7 percent confidence level, we determine the number of averages for each measurement (N) by dividing the allowance for data variation by the three-sigma value for that bandwidth and then squaring the result. N is rounded up to the nearest integer.

In this example, ECP starts to lose its advantage over the burst power measurement as the loop bandwidth approaches 100 Hz. However, in the case of a system with “No ALC,” ECP has a 15-fold advantage over the burst power measurement.

“No ALC” is not a trivial case. It effectively represents the case if a polar modulation scheme is used to impose modulation. In these schemes, the modulating signal is resolved into phase and amplitude components. Phase modulation is applied through the phased locked loop (PLL) in the synthesizer and amplitude modulation using ALC feed-forward techniques. With these ALC arrangements, the amplitude modulation is no longer regarded by the loop as a disturbance that it must act to remove—this represents the “No ALC” case. In summary we see that some characterization of a phone is necessary to determine the number of required averages. However, we can substantially improve measurement speed in most cases by using ECP.

Modulation Accuracy Measurement

The key modulation accuracy parameters and their system specifications include the following:

- maximum RMS EVM < 9 percent
- average peak EVM < 30 percent
- 95th percentile EVM < 15 percent
- frequency error < 0.1 ppm
- average origin offset suppression > 30 dB

We will focus on the RMS EVM (error vector magnitude) parameter. The noise-like nature of the 8PSK modulation format and a specification requirement that the maximum value is determined from 200 bursts makes RMS EVM problematic, in the manufacturing test environment—such a large number of bursts may take several seconds.

The question is, can we determine the statistics of RMS EVM for the device under test that will allow us to predict the likelihood of a given peak value being exceeded? The next few diagrams describe how the probability density function of the RMS EVM can be determined if we make the assumption that the error component in the signal is due to AWGN.

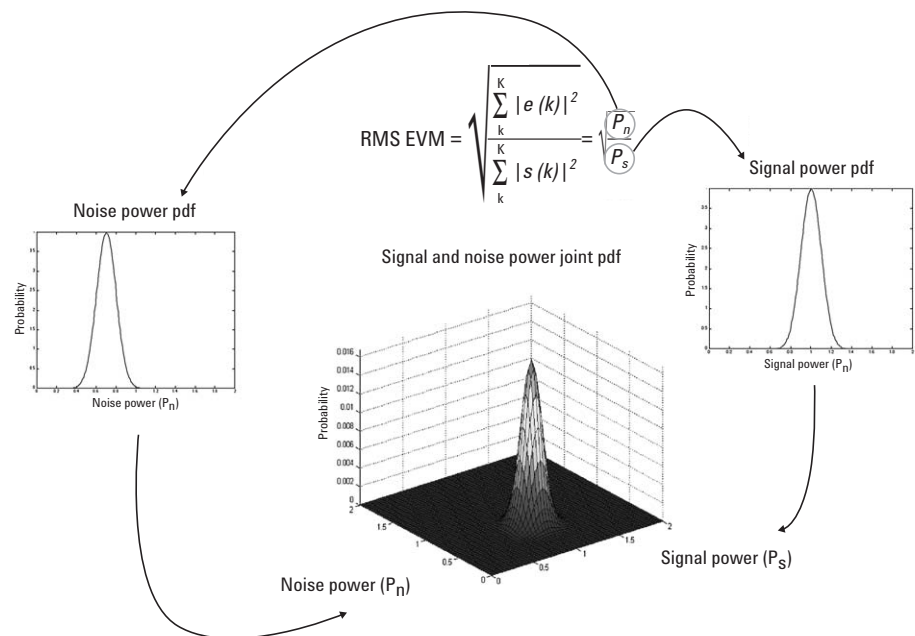


Figure 17. RMS EVM definition

The standards define RMS EVM as the square root of the ratio of error vector (noise) power to signal vector power.

We can generate a three-dimensional plot illustrating the joint distribution of average noise power and average signal power. Note that both the average noise power and the average signal power values tend towards the normal distribution and thus have Gaussian models.

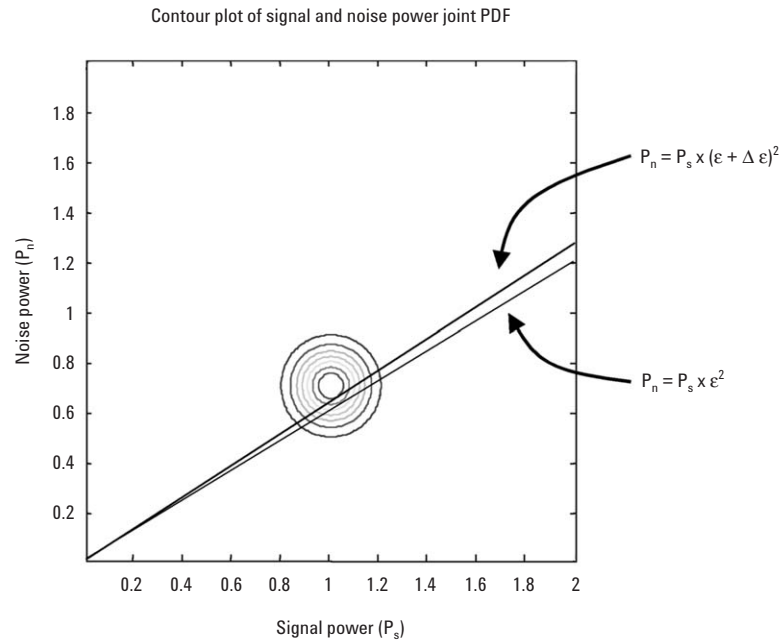


Figure 18. Determining the PDF of RMS EVM

With these concepts in mind, we can calculate the RMS EVM distribution mathematically.

In Figure 18 we see the joint probability distribution function (PDF) of the average signal power and average error power represented as a contour plot. We are looking down on the three-dimensional model shown in Figure 17. Each circle (contour) joins points of equal probability.

If we consider a given value of RMS EVM, ϵ , in a rectangular coordinate system defined by P_s and P_n , we see that the square of ϵ represents the slope of a line passing through the origin. This follows from the definition of RMS EVM.

Next, we consider a second RMS EVM value, $\epsilon + \Delta\epsilon$. The square of this value also represents the slope of a line passing through the origin. If we then integrate the volume lying under the joint PDF surface and bounded by these two lines, we can determine the probability of the RMS EVM lying between the two values ϵ and $\epsilon + \Delta\epsilon$.

By considering a range of values for ϵ stepped by $\Delta\epsilon$, we can determine a histogram that shows the distribution of RMS EVM values for a given set of signal power and error power statistics. As $\Delta\epsilon$ approaches zero, the histogram will become the PDF of the RMS EVM.

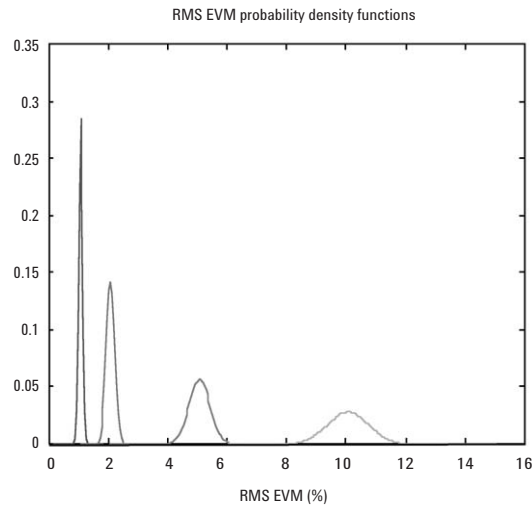


Figure 19. RMS EVM probability density functions

Figure 19 shows the RMS EVM PDF that we would expect when the noise is added white Gaussian noise (AWGN) for different values of signal-to-noise (SNR) ratio.

If we do the math for different SNR values we can generate a family of RMS EVM PDFs. It is notable that as the mean value of the RMS EVM increases, so does the spread of the distribution.

This is a useful observation. It means that the RMS EVM PDF is defined entirely by the average value. The standard deviation, or measure of spread, is a function of the average value. There are well established techniques for estimating average values from small sample sizes.

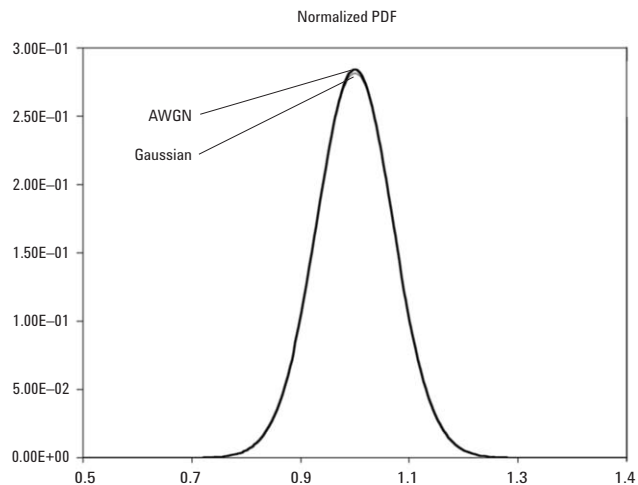


Figure 20. Normalized RMS EVM PDF

Two plots are shown in Figure 20. One is the normalized RMS EVM PDF of our signal with noise added; in this case the noise source is AWGN. The other plot is a true Gaussian distribution. The two appear to be very closely matched, although in reality there is some divergence around the mean and, although not visible here, at the tails. Because we are interested in estimating the probability of a peak value occurring, the Gaussian or normal distribution is not an accurate model.

In reality, the shape factor of our PDF is determined by several factors—the randomness of the data pattern in the signal, the EDGE transmit filter, the measurement filter, and the bandwidth of the AWGN. The effect of the AWGN bandwidth becomes negligible if the AWGN bandwidth exceeds the measurement filter bandwidth. The only requirement is that the additive noise has a flat noise spectral density over the measurement filter bandwidth.

This leads us to further consider what the distribution might look like for a signal in compression, which is a common source of distortion. For example, what happens if, instead of having a full 3.2 dB of overhead, we only have 3 dB of overhead in our power amplifier at the maximum power, and at the instantaneous peaks we get some compression on the signal?

In the code domain—the domain of waveform quality—we discover that the behavior of the compressed signal is somewhat better than our “pure” signal with randomly generated noise.

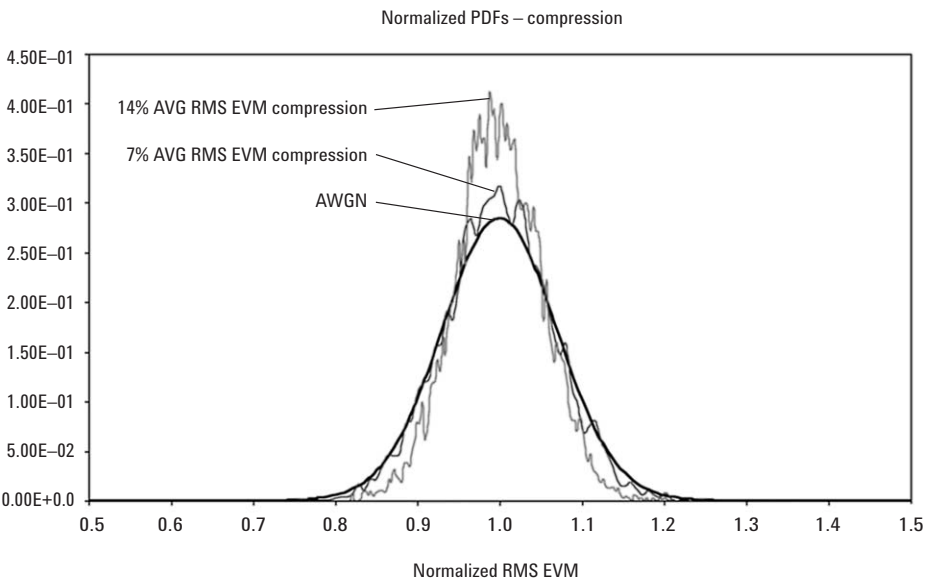


Figure 21. RMS EVM PDF for signals in compression

For measurements made on a real device in different degrees of compression, we plot the normalized PDFs atop the normalized PDF predicted by the model developed for an AWGN error signal.

A close examination shows us that for all values of average RMS EVM compression, the spread is always less than the spread predicted by the model developed for an AWGN error signal. Further, as the compression increases, the spread reduces.

This tells us that the model developed for an AWGN error signal can be regarded as the limiting case. If we assume this model, we can be sure that the peak value of RMS EVM for a signal in compression will be less than this value—whatever the degree of compression.

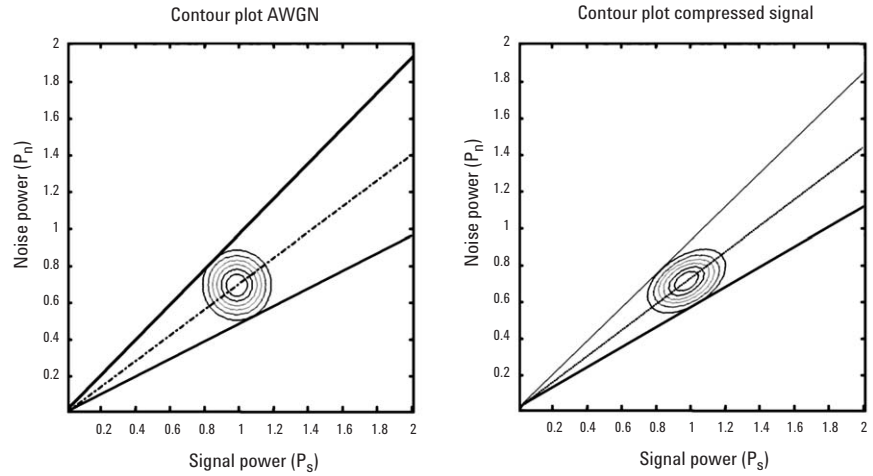


Figure 22. Contour plots for AWGN and signals in compression

Comparing the contour plots for AWGN and our compressed signal, Figure 22 illustrates why the model developed for an AWGN error signal can be regarded as a limiting case.

For both signals, the average RMS EVM values are the same, shown by the dotted lines. In the case of an AWGN error signal, because the noise power is not correlated to the signal power, the P_n and P_s values are evenly distributed about the mean, and thus the contours in the plot are circular.

In the case of the compressed signal, the noise power is correlated to the signal power: when signal power is high, we are more likely to see a large noise power. This tends to stretch the joint PDF along the dotted line that defines the average value. Since the total volume under the surface must remain one, the distribution is effectively pulled towards the average value.

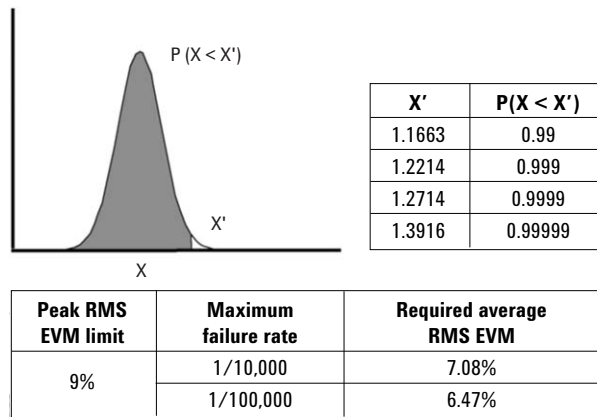


Figure 23. Tabulated values for the RMS EVM PDF

Figure 23 shows the probabilities for some offsets of the normalized RMS EVM PDF.

The tables tell us that if we require less than one failure in 10,000 phones tested, and if our specification limit for peak RMS EVM is 9 percent, the average RMS EVM value must be less than 7.08 percent. If we require less than one failure in 100,000, the average RMS EVM must be less than 6.47 percent. Therefore, if we find that the average of a small number of burst RMS EVM values is 6.47 percent or less, we can be confident that over 200 bursts of our phone will not exceed the 9 percent peak value limit. We are able to shorten the measurement time using statistical techniques to predict the performance of the phone—a significant improvement in a production test environment.

IQ Modulator Tuning

Now let us consider the in-phase/quadrature-phase (IQ) modulator.

IQ modulation generally is done at an intermediate frequency and then up-converted by means of an oscillator and amplifiers in the phone. Although the IQ modulator operates down at the IF, it is still imprecise enough to require some tuning on each device. This tuning process is required on every phone as part of the manufacturing test process. Traditionally IQ tuning has been done using special test modes on the phone.

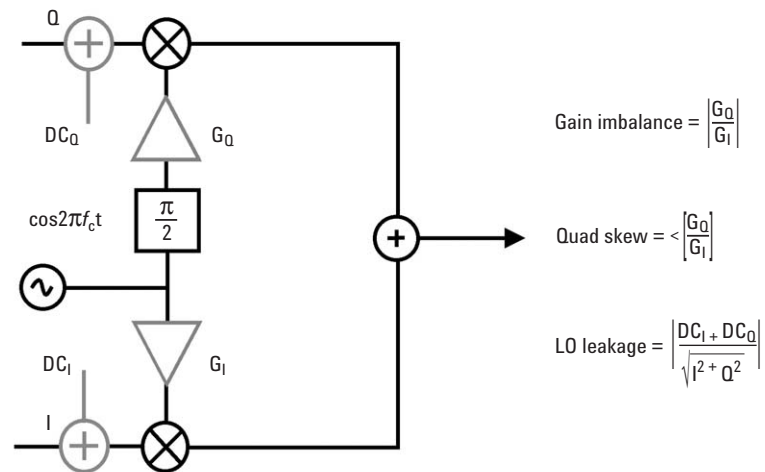


Figure 24. IQ modulator imbalance

In an IQ modulator, the carrier, which is the $\cos(2\pi f_c \tau)$ term, becomes the carrier for the in-phase (I) channel. When it is rotated 90 degrees to make $\sin(\omega\tau)$, it becomes the carrier for the quadrature (Q) channel. Thus the carriers are 90 degrees out of phase.

An ideal IQ modulator would consist simply of two perfect mixers, a perfect 90 degree phase shifter, and a perfect summing block. In an actual system none of these elements is perfect, and they contribute to distortion of the signal.

The imperfections can be modeled by additional gain stages in the I and Q channels. The gain stages are characterized as having a gain and phase shift at the carrier frequency plus a DC offset.

In practice, we use compensation circuits to drive gain imbalance toward a value of one, and quadrature skew and LO leakage toward values of zero.

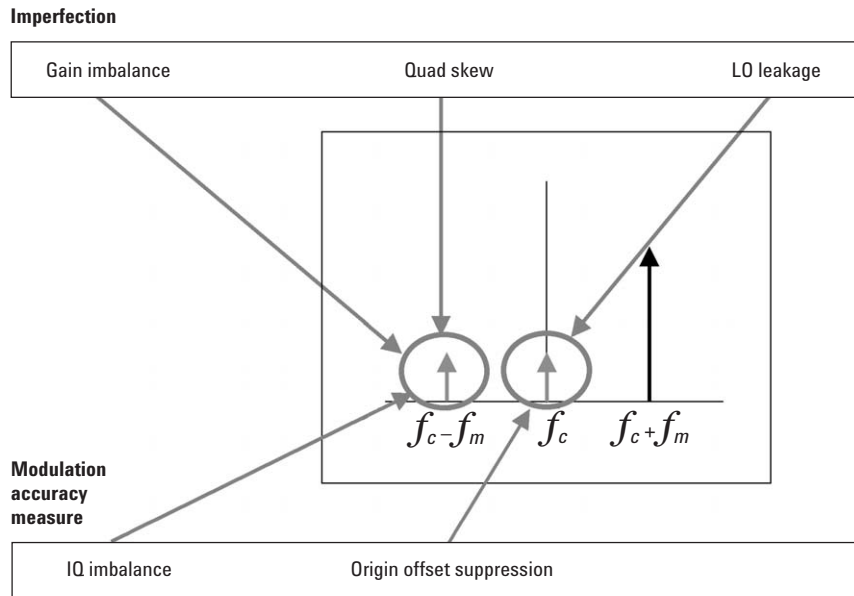


Figure 25. IQ tuning

The classical way of tuning an IQ modulator uses a CW signal. If we apply two sine waves, of frequency f_m and 90 degrees apart, to the I and Q channels, we should produce a sine wave at frequency $f_c + f_m$ if the IQ modulator is properly adjusted.

Looking at the output on a spectrum analyzer, shown in Figure 25, we can see the desired signal. However, we also see other frequency terms that reflect the imperfections of the IQ modulator. LO leakage causes the LO frequency to appear. Gain imbalance and quadrature skew together allow an image frequency ($f_c + f_m$) to appear.

We can tune the IQ modulator, usually through iteration, by setting the DC-offset, quadrature, and gain adjustments to minimize the LO frequency and image frequency components. This technique is effective, but it does require that our phone have a special test mode for generating the required sine waves on the I and Q channels.

It is clearly preferable to have a tuning technique that does not require a special test mode, but rather uses a normally-modulated burst. The algorithm defined in the standards for estimating parameters in the modulation measurement lends itself to such a technique. Because LO leakage is equivalent to the origin offset suppression, that measure exists already. By making a change to the parameter estimation algorithm, we also can determine the amplitude of the image frequency—the measure we refer to as the IQ imbalance.

Agilent has implemented this technique in its test sets to eliminate the need for any specialized test mode or test signal. We can run our phone in a normal loopback test mode, and without any knowledge of the modulation pattern, and the test set can extract the origin offset and image signal of the modulation. Without having to change modes or leave the domain of waveform quality, we can make the required measurements accurately and efficiently—a boost to our manufacturing throughput.

Test Modes

The ETSI standard defines three modes for testing mobile devices, all of which are supported in Agilent 8960 Series 10 test sets.

- **ETSI Test Mode A** is used for transmitter testing only. It turns on the transmitter allowing us to evaluate both the GMSK and 8PSK transmit signal; however, no data is received back from the test set.
- **ETSI Test Mode B** is a loop-back method of testing in which data sent on the downlink is sent back on the uplink. Data is looped back after the channel decoder stage. This mode can be used for GMSK and 8PSK transmitter testing as well as receiver BER for GPRS.
- **EGPRS Radio Block Loopback Mode** was created for testing EGPRS receiver BER. It also supports GMSK and 8PSK transmitter tests.

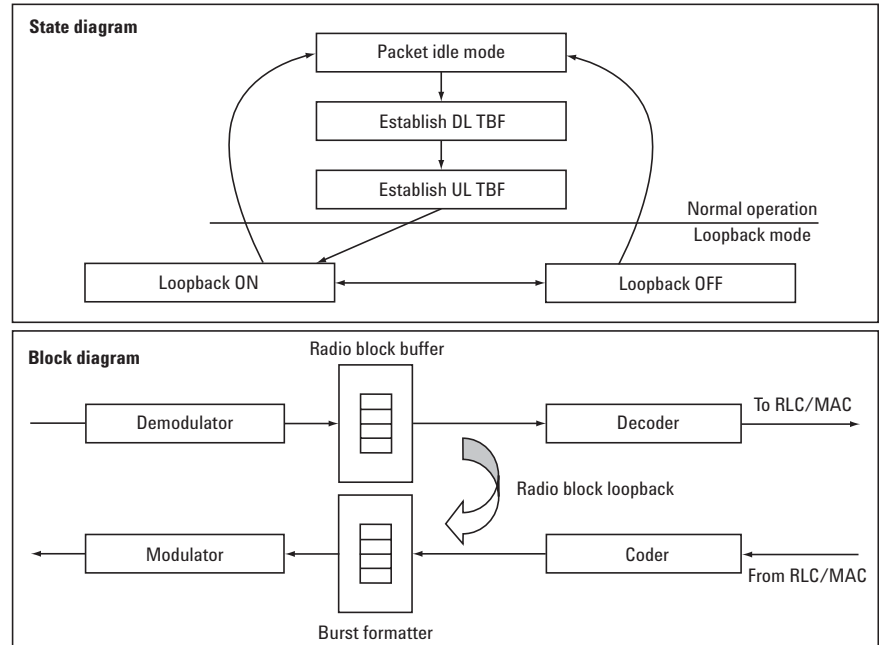


Figure 26. Switched radio block loopback mode

In the state diagram in Figure 26 see how the EGPRS switched radio block loopback mode is turned on to perform testing. First, downlink and uplink TBFs are established in the usual manner. A test mode command is sent to the mobile, forcing it into the Test Loopback ON sub-state. The test mode is terminated using the normal packet TBF release mechanism.

Perhaps the most common use of the loopback mode is illustrated in the lower block diagram of Figure 26. We send an RF signal into the radio demodulator but, in addition to decoding the signal and sending it to the upper layers to handle the packet information, we also strip off the raw data and send it in a burst to the channel decoder—at the same time re-modulating the transmitter signal of the phone itself. This process is used typically to test the receiver part of the phone, though we can measure the transmitter as well.

To measure the performance of the demodulator, we hunt for errors in the demodulation, which requires sending an impaired signal to the phone. Typically we make the impaired signal quite small, so that the phone is right at the limit of its ability to receive the signal. The signal coming back from the phone into the test set will be extremely high, since there are no other phones on the air interface. This returning signal will therefore be well above the noise floor and free from return-path errors. Our test set will be able to demodulate the signal easily, and any errors it detects will be attributable to the phone's demodulation process.

Summary

The need for speed in communications has driven the adoption of 8PSK modulation format for EDGE and its major variant, EGPRS. However, the need for speed in manufacturing is driving the adoption of new techniques for testing 8PSK, given this modulation format's noise-like nature.

Power measurement is one of the challenges introduced by 8PSK modulation. Estimated carrier power is a new technique that improves measurement speed without compromising accuracy.

Noise measurement is at the heart of the peak RMS EVM measurement. The statistics generated from this measurement give rise to a method for determining the peak value of RMS EVM from the average RMS EVM value.

IQ modulator testing is required on all phones. The IQ imbalance measure forms the basis of a method for tuning IQ modulators without having to place the phone in a special test mode.

ETSI defines three test modes to support mobile phone testing. A new EGPRS loopback test mode in particular allows for testing of 8PSK transmitters and receivers.

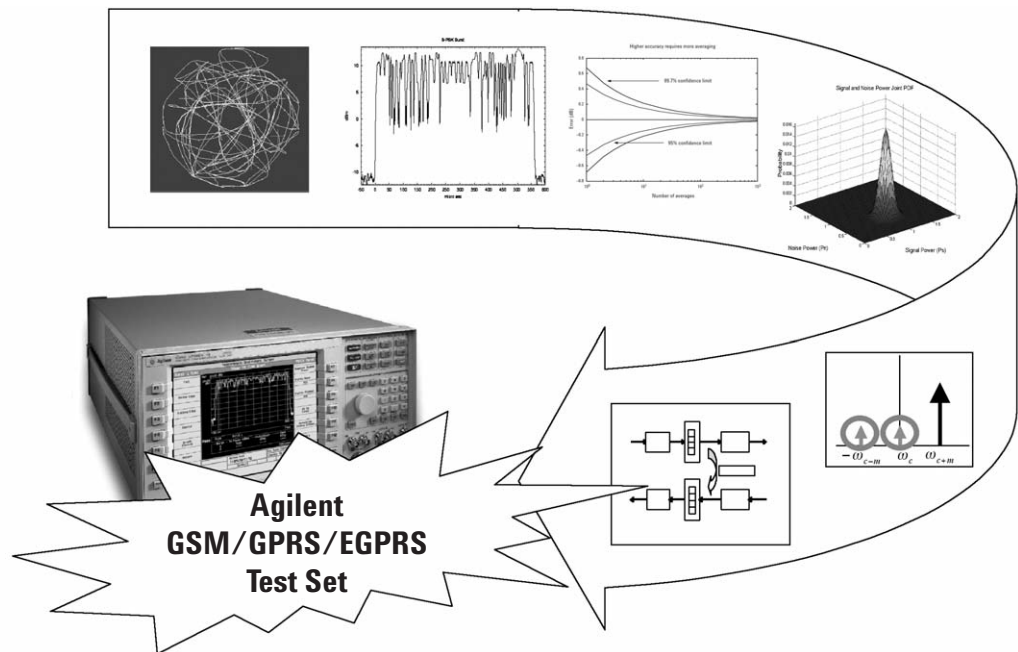


Figure 27. Agilent's 8960 Series 10 test set and test applications support GSM, GPRS, and now EGPRS

Agilent supports all of these measurements and test modes in what we call the “test application” versions of the 8960 Series 10 test set. Test applications are generally aimed at a manufacturing environment where throughput is of utmost importance. We also have a version of the product called the “lab application,” which includes all of the measurement techniques discussed in this paper, as well as additional RF capabilities.

Both the manufacturing test applications and the lab applications feature network connectivity, so that users can connect the test set to a LAN port and to the Internet. This connectivity makes it possible to send real data from the Internet through the Agilent test set which replicates all of the upper layer protocols as needed to emulate a live network and send data to the phone by means of a real RF link.

Additional capability lets users vary the coding parameters, time slot structure, and power to do a thorough evaluation of design technology with the phone connected to the network. A computer in the system can measure all the signaling, as well.

For more information on EGPRS testing and Agilent’s test solutions, please visit our Web site at **www.agilent.com/find/8960**.

Agilent Technologies' Test and Measurement Support, Services, and Assistance

Agilent Technologies aims to maximize the value you receive, while minimizing your risk and problems. We strive to ensure that you get the test and measurement capabilities you paid for and obtain the support you need. Our extensive support resources and services can help you choose the right Agilent products for your applications and apply them successfully. Every instrument and system we sell has a global warranty. Two concepts underlie Agilent's overall support policy: "Our Promise" and "Your Advantage."

Our Promise

Our Promise means your Agilent test and measurement equipment will meet its advertised performance and functionality. When you are choosing new equipment, we will help you with product information, including realistic performance specifications and practical recommendations from experienced test engineers. When you receive your new Agilent equipment, we can help verify that it works properly and help with initial product operation.

Your Advantage

Your Advantage means that Agilent offers a wide range of additional expert test and measurement services, which you can purchase according to your unique technical and business needs. Solve problems efficiently and gain a competitive edge by contracting with us for calibration, extra-cost upgrades, out-of-warranty repairs, and onsite education and training, as well as design, system integration, project management, and other professional engineering services. Experienced Agilent engineers and technicians worldwide can help you maximize your productivity, optimize the return on investment of your Agilent instruments and systems, and obtain dependable measurement accuracy for the life of those products.



Agilent Email Updates

www.agilent.com/find/emailupdates

Get the latest information on the products and applications you select.

Agilent T&M Software and Connectivity

Agilent's Test and Measurement software and connectivity products, solutions and developer network allows you to take time out of connecting your instruments to your computer with tools based on PC standards, so you can focus on your tasks, not on your connections. Visit **www.agilent.com/find/connectivity** for more information.

For more information on Agilent Technologies' products, applications or services, please contact your local Agilent office. The complete list is available at:

www.agilent.com/find/contactus

Phone or Fax

United States:

(tel) 800 829 4444
(fax) 800 829 4433

Canada:

(tel) 877 894 4414
(fax) 800 746 4866

China:

(tel) 800 810 0189
(fax) 800 820 2816

Europe:

(tel) 31 20 547 2111

Japan:

(tel) (81) 426 56 7832
(fax) (81) 426 56 7840

Korea:

(tel) (080) 769 0800
(fax) (080)769 0900

Latin America:

(tel) (305) 269 7500

Taiwan:

(tel) 0800 047 866
(fax) 0800 286 331

Other Asia Pacific Countries:

(tel) (65) 6375 8100
(fax) (65) 6755 0042

Email: tm_ap@agilent.com

Contacts revised: 1/12/05

Product specifications and descriptions in this document subject to change without notice.

© Agilent Technologies, Inc. 2005
Printed in USA, February 28, 2005
5989-1777EN



Agilent Technologies